Journal of Organometallic Chemistry 799-800 (2015) 299–310

Contents lists available at ScienceDirect

Journal of Organometallic Chemistry

journal homepage: www.elsevier.com/locate/jorganchem

Synthesis and comparative behavior of ruthena(II)cycles bearing benzene ligand in the radical polymerization of styrene and vinyl acetate

Vanessa Martínez Cornejo [a, b], Jessica Olvera Mancilla [a], Salvador López Morales [a], José Alberto Oviedo Fortino [b], Simón Hernández-Ortega [b], Larissa Alexandrova [a, **], Ronan Le Lagadec [b, *]

[a] Instituto de Investigaciones en Materiales, UNAM, Circuito Exterior s/n, Ciudad Universitaria, 04510 México D. F., Mexico
[b] Instituto de Química, UNAM, Circuito Exterior s/n, Ciudad Universitaria, 04510 México D. F., Mexico

ARTICLE INFO

Article history:
Received 30 August 2015
Received in revised form
5 October 2015
Accepted 8 October 2015
Available online 22 October 2015

Keywords:
Cyclometalated ruthenium complexes
Ligand exchange
Atom transfer radical polymerization

ABSTRACT

A series of half-sandwich ruthenium(II) complexes of the type $[Ru(\eta^6\text{-}C_6H_6)(N\cap C)L]PF_6$ (L = PPh_3, P(*n*-Bu)$_3$, $SbPh_3$, MeCN), bearing cyclometalated *N*,*N*-dimethylbenzylamine (**1a**–**d**) and 2-phenylpyridine (**2a**–**d**) moieties, has been efficiently prepared by ligand substitution. The molecular structures of the new compounds were unequivocally determined by single-crystal X-ray diffraction. The catalytic activity of the complexes in the radical polymerizations of styrene and vinyl acetate was evaluated, and a comparative structure – activity analysis was performed.

1. Introduction

Cyclometalation of ligands by transition metals is one of the easiest ways to form organometallic compounds with a metal-carbon sigma bond. Due to the stabilization by chelation, these compounds are generally quite robust and therefore may easily be managed without extreme precautions. The platinum group metals are by far the most popular domain used for cyclometalation reactions and a vast number of metallocycles has been prepared by heteroatom-assisted C–H bond activation, with the palladium complexes being the most studied, since cyclopalladated derivatives are known for nearly all classes of ligands [1–4]. The corresponding ruthenium compounds have been much less investigated and their synthesis and properties are less well understood, even though ruthenacycles have shown remarkable photophysical and electrochemical properties. For instance, they have been considered as promising materials for applications in solar cells, intervalence electron-transfer systems or in bio-electronic devices as efficient electron shuttles for oxidoreductase enzymes [1,2,5–11]. The organoruthenium derivatives also possess the required characteristics for the interaction with biomolecules and several ruthenacycles are considered as promising candidates for anticancer drugs [1,12–14]. Although ruthenium complexes have been widely investigated for homogeneous catalysis, their *ortho*-metalated counterparts have not as yet demonstrated their full potential in this area and only a few examples of cyclo-ruthenated compounds showing good activity in homogeneous catalysis have been reported [15–17].

Cycloruthenation is very versatile and of broad scope mostly because of the great diversity and availability of ruthenium precursors. However, one setback is the relative lack of reactivity of ruthenium complexes toward the cyclometalation reaction and frequently the synthetic route requires various steps and results in low yields [1,18]. Our group has been studying the synthesis and possible ways of application of cycloruthenated compounds for almost two decades. Simple and highly effective synthesis of ruthenacycles has been developed which allows easy modification

Abbreviations: BEB, 1-(bromoethyl)-benzene; MMA, methyl methacrylate; St, styrene; VAc, vinyl acetate; MEK, methyl ethyl ketone; TEMPO, (2,2,6,6-tetramethyl-piperidin-1-yl)oxyl; Cyclometalated ligands: dmba, *N*,*N*-dimethylbenzylamine; phpy, 2-phenylpyridine; tolpy, 2-(*p*-tolyl)pyridine.

* Corresponding author.
** Corresponding author.
E-mail addresses: laz@unam.mx (L. Alexandrova), ronan@unam.mx (R. Le Lagadec).

http://dx.doi.org/10.1016/j.jorganchem.2015.10.013
0022-328X/

of the compounds in the desirable direction [8,9,19–21].

One of the promising applications of the ruthenacycles in catalysis may be in atom transfer radical polymerization (ATRP) or metal catalyzed living radical polymerization. Indeed, ruthenium(II) complexes were among the first catalysts reported for this reaction and to the date remain one of the most active and versatile catalytic systems [22,23]. Moreover, ruthenium complexes have been known to be among the most efficient for C–C bond formation in the Karasch addition or atom transfer radical addition (ATRA), a reaction mechanistically very similar to ATRP [24–26]. The classical mechanism of ATRP consists in the reversible homolysis of a terminal carbon-halogen bond of the dormant species through the abstraction of the halogen atom by the metallic catalyst resulting in the formation of growing radicals and the complex in +1 higher oxidation state (Scheme 1). The complex participates in a reversible oxidative addition reaction and therefore its catalytic activity should correlate with its redox potential, where a lower redox potential means higher catalytic activity. A direct correlation has been shown for structurally simpler copper catalysts [27], while the structure – ATRP reactivity relationship for the ruthenium-based catalysts is highly sophisticated and no simple dependence has been found, even for structurally similar ruthenium compounds [28–30]. Cyclometalated ruthenium(II) complexes may have advantages here in comparison with their coordinated congeners because of the less positive Ru^{III}/Ru^{II} potential [1,12,31–33]. Several ruthenacycles have been reported as efficient catalysts in ATRP and ATRA reactions of different acrylic and vinylic compounds [26,30,34–36]. They may be better referred to catalyst precursors since all of them are 18 electrons coordinatively saturated molecules and a vacant site must be generated to enable their activation for ATRP [30,34–36]. Recently, the very active catalyst precursor [Ru(η^6-C_6H_6)(dmba)(MeCN)]PF_6 has been reported, which was able to polymerize vinyl acetate, one of the most difficult monomers for ATRP, via the reversible activation of the carbon-Cl terminals under specific conditions [37]. Additionally, the investigation demonstrated the importance of the presence of a benzene ligand in the structure of the catalyst, since the complexes having benzene were generally more active than their counterparts with polypyridine ligands. Unfortunately, polymerization of other more conjugated monomers, such as styrene or methyl methacrylate proceeded without control.

To continue our effort in understanding the role of potentially labile ligands in the catalytic activity, a series of ten cyclometalated ruthenium(II) complexes bearing η^6-C_6H_6 has been prepared (See Fig. 1 for the structures). In order to evaluate the influence of different parameters such as the lability of the ligands and the electron density on the metal centre, the structure of the complexes was gradually modified: (i) two different cycloruthenated moieties, *N*,*N*-dimethylbenzylamine (group **1**) and 2-phenylpyridine (group **2**) were introduced, and, (ii) a substitution reaction allowed the incorporation of various ancillary ligands such as acetonitrile, phosphines and stibines. Such a variety of compounds enabled the investigation of the influence of the different ligands on the catalytic activity and to clarify some mechanistic aspects. The behavior of the complexes was analyzed under conditions of the polymerization of St and VAc. Furthermore, considering that the ionic character of the complexes may also impact on their catalytic performance [26,38,39], two neutral [Ru(η^6-C_6H_6)(N∩C)Cl] compounds (group **3**), with a phpy-based cyclometalated fragment, were also studied and the results compared with group **1** and **2** catalysts.

2. Experimental

2.1. Materials and reagents

All reactions were carried out under inert atmosphere (dinitrogen or argon) using conventional Schlenk glassware; all solvents were dried using established procedures and distilled under dinitrogen prior to use. Styrene (99%) was washed three times with 1 wt % NaOH solution and passed through a column filled with neutral alumina, vinyl acetate (>99%, Aldrich) was passed through a neutral alumina column, distilled under reduced pressure, and stored under nitrogen. All the others reagents were purchased from Aldrich and used as received: *N*,*N*-dimethylbenzylamine, 2-phenylpyridine, *n*-decane, BEB (97%), carbon tetrachloride, tetrahydrofuran HPLC, tri-*n*-butylphosphine, triphenylphosphine, triphenylstibine, potassium hexafluorophosphate, silver hexafluorophosphate, anhydrous ether and anhydrous acetonitrile. Commercial $RuCl_3$ was purchased from Pressure Chemical Company. Complexes **1d**, **3′**, **3″** and **4** were prepared according to the literature [18,19,40–42].

Mass Spectra were obtained using a JEOL JMS-SX102A instrument with *m*-nitrobenzyl alcohol as the matrix [FAB^+ mode, *m*/*z* (%,

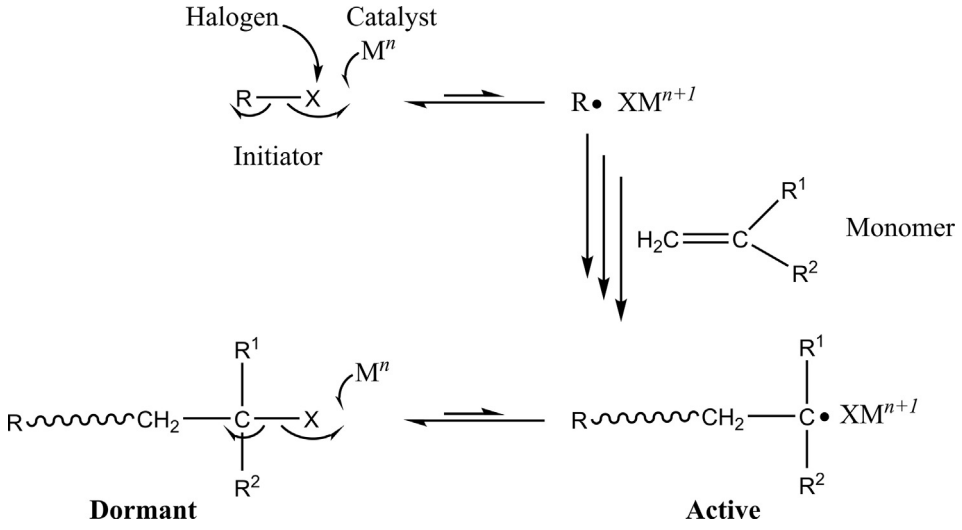

Scheme 1. Mechanism of ATRP.

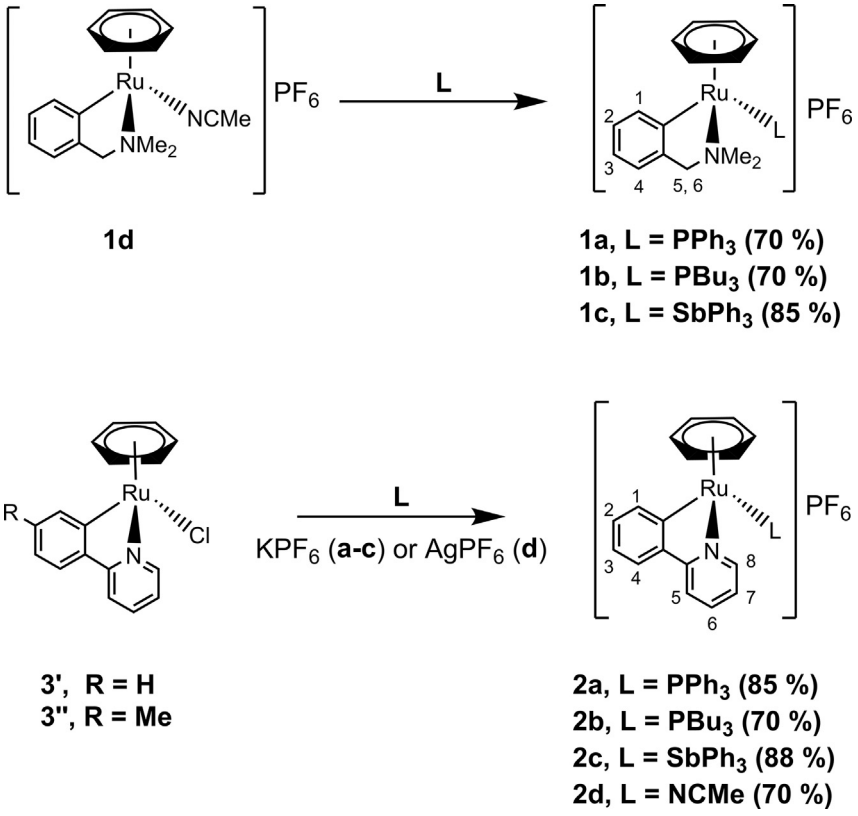

Fig. 1. Synthetic routes, structures of ruthenacycles and numbering scheme for NMR assignation used in the present study.

relative abundance) throughout]. Infrared spectra were recorded on an Alpha ATR spectrometer from Bruker. ^{1}H (300 MHz) and $^{31}P\{^{1}H\}$ (121.6 MHz) NMR spectra were recorded using a JEOL GX instrument. The δ scale is used throughout; chemical shifts are in ppm, and the coupling constants are in Hz. Elemental analyses were obtained on an Exeter Analytical CE-440.

Conversions were determined from the concentration of residual monomer measured by GC using a Shimadzu GC-2010 gas chromatograph equipped with one capillary column RESTEK stabilwax (30 m, 0.53 mm ID, and 0.5 μmdf) with *n*-decane as an internal standard in every polymerization. Analysis conditions were as follows: injector temperature, 220 °C; temperature program, 4 min 40 °C, 15 °C/min until 220 °C, 2 min 220 °C. Molecular weights (M_n) and molecular weight distributions (M_w/M_n) of the polymers were determined using a gel permeation chromatograph Waters 2695 ALLIANCE Separation Module, equipped with two HSP gel columns in series (HR MBL molecular weight range from 5102 to 7105 and MB-B from 103 to 4106) and a RI Waters 2414 detector. THF was used as an eluent at 35 °C with a flow rate of 0.5 mL/min. Linear polystyrene standards were used for the calibration. Theoretical molecular weights were calculated without taking into account the end groups according to the following equation: $M_{n,th} = ([Monomer]_0/[Initiator]_0) \times Conversion \times MW_{monomer}$, where $0 \leq conversion \leq 1$.

GC-MS analysis were performed on a Shimadzu GC-2010/MS-QP2010s system equipped with an AOC-20i auto sampler, with injector temperature of 320 °C, a 1:5 split ratio and injection volume of 1 μL. Capillary column separation was a 0.25 μm thick film [30 m x 0.32 mmID Rtx®-5MS (RESTEK) with a 5 m integra-guard column] using a flow rate of 1.21 mL/min and 70 kPa helium pressure. The chromatograms were acquired in the electron impact scan mode at 70 eV with a mass range of 40–900 (*m*/*z*). The data were acquired and processed using Shimadzu GC-MS solution software.

2.2. Crystallography

Crystalline yellow prisms for **1a**–**1c**, and **2a**–**2d** were grown independently from CH_2Cl_2/diethyl ether and mounted on glass fibers. In all cases, the X-ray intensity data were measured at 298 K on a Bruker SMART APEX CCD-based X-ray diffractometer system equipped with a Mo-target X-ray tube ($\lambda = 0.71073$ Å). The detector was placed at a distance of 5.0 cm from the crystals in all cases. A total of 1800 frames were collected with a scan width of 0.3 in ω and an exposure time of 10 s/frame. The frames were integrated with the Bruker SAINT Software package using a narrow-frame integration algorithm [43]. The integration of the data was done using a triclinic unit cell for **1b**, orthorhombic for **2d** and monoclinic for **1a**, **1c**, **2a**, **2b**, **2c**, to yield a total of 24735 for **1a**, 13676 for **1b**, 25448 for **1c**,125407 for **2a**, 25286 for **2b**, 35321 for **2c** and 23295 for **2d** reflections to a maximum 2θ angle of 50.00, of which 5529 [R(int) = 0.0579], 6006 [R(int) = 0.0324], 5785 [R(int) = 0.0797], for **1a** – **1c**, 5678 [R(int) = 0.0645], 5696 [R(int) = 0.0898], 5973 [R(int) = 0.0940], 3804 [R(int) = 0.0583] for **2a** – **2d** were independent. Analysis of the data showed in all cases negligible decays during data collections. The structures were solved by Patterson method using SHELXS-2012 program [44]. The remaining atoms were located via a few cycles of least squares refinements and difference Fourier maps. Hydrogen atoms were input at calculated positions, and allowed to ride on the atoms to which they are attached. Thermal parameters were refined for hydrogen atoms on the phenyl groups using a Ueq = 1.2 Å to precedent atom in all cases. For all complexes, the final cycle of refinement was carried out on all non-zero data using SHELXL-

2014/7 [44]. The PF_6 anion in all compounds, the CH_2Cl_2 solvent in compound **1b** and the arene ring in compounds **2b** and **2d** are disordered and were refined in two major contributors and refined anisotropically.

2.3. General procedure for complexes 1

In a typical experiment, a solution of **1d** (200 mg, 0.40 mmol) and 0.6 mmol of the ligand (**1a** triphenylphosphine, **1b** tri-*n*-butylphosphine or **1c** triphenylstibine) in 30 mL of MeOH was stirred for 20 h at 45 °C. The solvent was evaporated under vacuum, and the residue was dissolved in CH_2Cl_2. The solution was passed through a short column of Al_2O_3 using CH_2Cl_2 as an eluent. A pale yellow fraction was collected and evaporated to dryness. Crystallization from CH_2Cl_2/diethyl ether (slow diffusion) gave yellow crystals, which were washed with diethyl ether and dried under vacuum.

2.3.1. Synthesis of 1a

2.3.1.1. Yield. 202 mg, 70%. ^{1}H NMR (CD_3CN): 8.04 (d, 1H, $^3J_{HH}$ = 8 Hz, H1), 7.61–7.30 (m, 15H, PPh_3), 7.16 (t, 1H, $^3J_{HH}$ = 7.2 Hz, H2), 6.98 (t, 1H, $^3J_{HH}$ = 7 Hz, H3), 6.63 (d, 1H, $^3J_{HH}$ = 7.5, H4), 5.60 (s, 6H, C_6H_6), 2.91 (s, 3H, NMe), 2.71 (s, 3H, NMe), 2.72 (d, 1H, $^2J_{HH}$ = 14 Hz, H5), 2.39 (d, 1H, $^2J_{HH}$ = 14, Hz, 2H, H6). ^{31}P{^{1}H} NMR (CD_3CN): 33.5 (s, PPh_3), −144.6 (stp, $^1J_{PF}$ = 704.25 Hz, PF_6). M/S FAB$^+$: 576 [(M + H) − PF_6] (18%), 498 [(M + H) − (C_6H_6 + PF_6)] (12%), 314 [(M + H) − (PPh_3 + PF_6)] (15%), 236 [(M + H) − (C_6H_6 + PPh_3 + PF_6)] (6%). IR (FTIR): υ 832 (PF_6, s). Anal. Calcd. for $C_{33}H_{33}F_6NP_2Ru$: C, 55.00; H, 4.62; N, 1.94. Found: C, 54.72; H, 4.65; N, 2.12.

2.3.2. Synthesis of 1b

2.3.2.1. Yield. 184 mg, 70%. ^{1}H NMR (CD_3CN): 7.79 (d, 1H, $^3J_{HH}$ = 9 Hz, H1), 7.11–6.85 (m, 3H, H2+H3+H4), 5.76 (s, 6H, C_6H_6), 3.59 (d, 1H, $^2J_{HH}$ = 12 Hz, H5), 3.31 (d, 1H, $^2J_{HH}$ = 12 Hz, H6), 2.93 (s, 3H, NMe), 2.74 (s, 3H, NMe), 1.84–1.53 (m, 6H, PBu_3), 1.43–1.20 (m, 12H, PBu_3), 0.90 (t, $^3J_{HH}$ = 6.8 Hz, 9H, PBu_3). ^{31}P{^{1}H} NMR (CD_3CN): 13.02 (s, PBu_3), −144 (stp, $^1J_{PF}$ = 704.6 Hz, PF_6). M/S FAB$^+$: 516 [(M + H) − PF_6] (100%), 438 [(M + H) − (C_6H_6 + PF_6)] (34%), 314 [(M + H) − (PBu_3 + PF_6)] (96%), 236 [(M + H) − (C_6H_6 + PBu_3 + PF_6)] (30%). IR (FTIR): υ 831 (PF_6, s). Anal. Calcd. for $C_{27}H_{45}F_6NP_2Ru{\cdot}0.5CH_2Cl_2$: C, 46.98; H, 6.59; N, 1.99. Found: C, 47.41; H, 6.51; N, 2.21.

2.3.3. Synthesis of 1c

2.3.3.1. Yield. 275 mg, 85%. ^{1}H NMR (CD_3CN): 8.05 (d, 1H, $^3J_{HH}$ = 6 Hz, H1), 7.53 (t, 3H, $^3J_{HH}$ = 7.5 Hz, H9), 7.44 (t, 6H, $^3J_{HH}$ = 7 Hz, H9), 7.32 (d, 6H, $^3J_{HH}$ = 7.5 Hz, H9), 7.16 (t, 1H, $^3J_{HH}$ = 7.5 Hz, H2), 6.96 (t, 1H, $^3J_{HH}$ = 7.5 Hz, H3), 6.69 (d, 1H, $^3J_{HH}$ = 7 Hz, H4), 5.79 (s, 6H, C_6H_6), 3.17 (d, 1H, $^2J_{HH}$ = 15 Hz, H5), 3.04 (s, 3H, NMe), 2.93 (d, 1H, $^3J_{HH}$ = 12 Hz, H6), 2.74 (s, 3H, NMe). ^{31}P{^{1}H} NMR (CD_3CN): −144 (stp, $^1J_{PF}$ = 706.5 Hz, PF_6). M/S FAB$^+$: 667 [(M + H) − PF_6] (12%), 589 [(M + H) − (C_6H_6 + PF_6)] (2%), 314 [(M + H) − ($SbPh_3$ + PF_6)] (45%), 236 [(M + H) − (C_6H_6 + $SbPh_3$ + PF_6)] (10%). IR (FTIR): υ 831 (PF_6, s). Anal.: Calcd. for $C_{33}H_{33}F_6NPRuSb$: C, 48.85; H, 4.10; N, 1.73; Found: C, 48.83; H, 4.10; N, 1.87.

2.4. General procedure for complexes 2a–c

In a typical experiment, a solution of **3'** (200 mg, 0.543 mmol), 0.815 mmol of ligand (**2a** triphenylphosphine, **2b** tri-*n*-butylphosphine or **2c** triphenylstibine) and NH_4PF_6 (177 mg, 1.086 mmol) in 30 mL of MeOH was stirred for 20 h at 45 °C. The solvent was evaporated under vacuum, and the residue was dissolved in CH_2Cl_2. The solution was passed through a short column of Al_2O_3 using CH_2Cl_2 as an eluent. A pale yellow fraction was collected and evaporated to dryness. Crystallization from CH_2Cl_2/diethyl ether (slow diffusion) gave yellow crystals, which were washed with diethyl ether and dried under vacuum.

2.4.1. Synthesis of 2a

2.4.1.1. Yield. 341 mg, 85%. ^{1}H NMR (CD_3COCD_3): 9.26 (d, 1H, $^3J_{HH}$ = 5.5, H8), 7.81 (d, 1H, $^3J_{HH}$ = 7.5, H1), 7.53 (t, 1H, $^3J_{HH}$ = 7.7 Hz, H2), 7.47–7.38 (m, 2H, H3 and H6), 7.32 (dd, 3H, $^3J_{HH}$ = 7.9 Hz, $^4J_{HH}$ = 6.1 Hz, H4, H5 and H7), 7.25–7.14 (m, 6H, PPh_3), 7.01–6.77 (m, 9H, PPh_3), 6.03 (s, 6H, C_6H_6). ^{31}P{^{1}H} NMR (CD_3COCD_3): 43.84 (s, PPh_3), −144.19 (stp, $^1J_{PF}$ = 707.8 Hz, PF_6). M/S FAB$^+$: 596 [(M + H) − PF_6] (82%), 518 [(M + H) − (C_6H_6 + PF_6)] (38%), 334 [(M + H) − (PPh_3 + PF_6)] (18%), 256 [(M + H) − (C_6H_6 + PPh_3 + PF_6)] (8%). IR (FTIR): υ 832 (PF_6, s). Anal.: Calcd.: $C_{35}H_{29}F_6NP_2Ru{\cdot}CH_2Cl_2$: C, 52.38, H, 3.78; N, 1.70. Found: C, 52.98; H, 3.82; N = 1.83.[1]

2.4.2. Synthesis of 2b

2.4.2.1. Yield. 368 mg, 70%. ^{1}H NMR (CD_3COCD_3): 9.23 (d, $^3J_{HH}$ = 5.8 Hz, 1H, H8), 8.18 (d, 1H, $^3J_{HH}$ = 8.1 Hz, H1), 8.06–7.91 (m, 3H, H2, H3 and H6), 7.26 (t, 1H, $^3J_{HH}$ = 7.3 Hz, H4), 7.21–7.12 (m, 2H, H5 and H7), 6.16 (s, 6H, C_6H_6), 1.53–1.11 (m, 18H, PBu_3), 0.8 (t, ^3J = 7.0 Hz, 9H, PBu_3). ^{31}P{^{1}H} NMR (CD_3COCD_3): 21.39 (s, PBu_3): −144 (stp, J = 706.6 PF_6). M/S FAB$^+$: 536 ([M + H] − PF_6]: (100%), 458 [(M + H) − (C_6H_6 + PF_6)] (28%), 334 [(M + H) − (PBu_3 + PF_6)] (18%), 256 [(M + H) − (C_6H_6 + PBu_3 + PF_6)] (19%). IR (FTIR): υ 832 (PF_6, s). Anal. Calcd. for $C_{29}H_{41}F_6NP_2Ru$: C, 51.17; H, 6.07; N, 2.06. Found: C, 51.26; H, 5.91; N, 2.08.

2.4.3. Synthesis of 2c

2.4.3.1. Yield. 397 mg, 88%. ^{1}H NMR (CD_3CN) 9.0 (d, 1H, $^3J_{HH}$ = 6 Hz, H8), 7.83 (d, 1H, $^3J_{HH}$ = Hz, H1), 7.56–7.35 (m, 6H, H2 to H7), 7.30–7.25 (m, 6H, $SbPh_3$), 7.05–6.9 (m, 9H, $SbPh_3$), 5.90 (s, 6H, C_6H_6). ^{31}P{^{1}H} NMR (CD_3CN): −143.99 (stp, $^1J_{PF}$ = 704.25 PF_6). M/S FAB$^+$: 687 [(M + H) − PF_6] (35%), 609 [(M + H) − (C_6H_6 − PF_6)] (1%), 334 [(M + H) − ($SbPh_3$ − PF_6)] (92%), 256 [(M + H) − (C_6H_6 + $SbPh_3$ + PF_6)] (25%). IR (FTIR): υ 830 (PF_6, s). Anal. Calcd. for $C_{35}H_{29}F_6NPRuSb{\cdot}0.5CH_2Cl_2$: C, 48.79; H, 3.46; N, 1.60. Found: C, 48.77; H, 3.47; N, 1.67.

2.5. Synthesis of 2d

A solution of complex **3'** (200 mg, 0.543 mmol) and $AgPF_6$ (137.4 mg, 0.543 mmol) in 25 mL of acetonitrile was stirred for 2 h at room temperature. The reaction mixture was filtered through Celite and the remaining pale yellow solution was evaporated to dryness. Crystallization from CH_2Cl_2/diethyl ether (slow diffusion) gave yellow crystals, which were washed with diethyl ether and dried under vacuum. Yield: 197 mg, 70%. ^{1}H NMR (CD_3CN): 9.24 (dd, 1H, $^3J_{HH}$ = 6 Hz, $^4J_{HH}$ = 2 Hz, H8), 8.17 (ddd, 1H, $^3J_{HH}$ = 8 Hz, $^4J_{HH}$ = 1.5, $^5J_{HH}$ = 0.6 Hz, H1), 7.94–7.90 (m, 2H, H3 and H5), 7.77 (dd, 1H, $^3J_{HH}$ = 8 Hz, $^4J_{HH}$ = 1.5 Hz, H7), 7.28–7.15 (m, 3H, H2, H4 and H6), 5.78 (s, 6H, C_6H_6), 2.16 (s, 3H, NCMe). ^{31}P{^{1}H} NMR (CD_3CN): −144 (stp, $^1J_{PF}$ = 704.25 Hz, PF_6). M/S FAB$^+$: 375[(M + H) − PF_6] (1%), 297 [(M + H) − (C_6H_6 + PF_6)] (2%), 334 [(M + H) − (NCMe + PF_6)] (32%), 256 [(M + H) − (C_6H_6 + NCMe + PF_6)] (8%). IR (FTIR): υ 827 (PF_6, s), 2261 (NCMe, w). Anal. Calcd. for $C_{19}H_{17}F_6N_2PRu$: C, 43.94; H, 3.30; N, 5.39. Found: C, 43.83; H, 3.22; N, 5.30.

[1] Although these results are outside the range viewed as establishing analytical purity, they are provided to illustrate the best values obtained to date.

2.6. Procedures for the polymerization reactions

2.6.1. Polymerization of styrene

All reactions were carried out in solution (St/MEK 50% v/v) under dinitrogen or argon atmosphere at 80 °C. The initial molar ratio of $[monomer]_0/[initiator]_0/[complex]_0$ was 200/1/1 with BEB used as initiator. A polymerization procedure was as follows: **3′** (50 mg, 0.135 mmol), BEB (18 μL, 0.135 mmol), St (3 mL, 27 mmol) or **3″** (50 mg, 0.13 mmol), BEB (18 μL, 0.13 mmol), St (3 mL, 27 mmol); MEK (3 mL) and *n*-decane (0.3 mL) were placed in a 25 mL Schlenk flask and degassed three times using pump-nitrogen cycles. The mixture was stirred for 10 min at room temperature until homogenous. The flask was immersed in an oil bath previously heated at 80 °C. Samples were removed after certain time intervals using degassed syringes. For the cationic complexes the procedure was as follows: **2a** (100 mg, 0.135 mmol), BEB (18 μL, 0.135 mmol), St (3 mL, 27 mmol), *n*-decane (0.3 mL) and MEK (3 mL) were placed in a 25 mL Schlenk flask and degassed three times using pump-nitrogen cycles. The mixture was stirred for 10 min at room temperature until homogenous, and 8 aliquots (0.75 mL each) were injected into baked glass tubes and sealed under nitrogen. The tubes were immersed in an oil bath previously heated at 80 °C. The polymerizations were stopped at the desired time by cooling the tubes in ice-cold water. Conversions were determined by GC and the polymer samples injected into GPC without purification.

2.6.2. Polymerization of vinyl acetate

The polymerization of VAc was performed as follows: complex **1b** (178 mg, 0.271 mmol), CCl_4 (26 μL, 0.271 mmol), VAc (5 mL, 54.2 mmol), *n*-decane (0.5 mL) and MEK (5 mL) were placed in a 25 mL Schlenk flask and degassed three times using pump-nitrogen cycles. The mixture was stirred for 10 min at room temperature until homogenous, and 8 aliquots (0.62 mL each) of solution were injected into baked glass tubes and sealed under nitrogen. The tubes were immersed in an oil bath previously heated at 80 °C. The polymerizations were stopped at the desired time by cooling the tubes in ice-cold water. Conversions were determined by GC and the polymer samples injected into GPC without purification.

3. Results and discussion

3.1. Synthesis

As mentioned above, the complexes used in the study could be divided into three principal groups based on the cyclometalated ligand, dmba (**1**) *vs* phpy (**2** and **3**), and on the charge, cationic (**1** and **2**) *vs* neutral (**3**) compounds. In addition, all complexes bear η^6 coordinated benzene, and four different donor ligands were introduced within the dmba and phpy series, as shown in Fig. 1, from relatively labile MeCN to more strongly bound phosphines and stibines [45]. The ligands were also chosen according to their steric and electronic properties, for instance bulkier PPh_3 and $SbPh_3$ *vs* MeCN and P(*n*-Bu)$_3$, or more labile stibine *vs* phosphine [45]. Additionally, two neutral ruthenacycles derived from phpy (**3′**) and tolpy (**3″**) were also used in the present study [40]. Complex **1d** can readily be prepared from the direct metalation of *N*,*N*-dimethylbenzylamine by the $[Ru(\eta^6\text{-}C_6H_6)Cl_2]_2$ dimer in acetonitrile, as reported by Pfeffer et al. [18]. Compounds **1a**–**c** were obtained in excellent yields (70–85%) from **1d** by substitution in methanol of the coordinated acetonitrile by more basic ligands such as triphenylphosphine (**a**) tri-*n*-butylphosphine (**b**) and triphenylstibine (**c**) [14].

Pfeffer also reported that the reaction between 2-phenylpyridine and the ruthenium dimer under the same conditions does not produce a clean reaction but a mixture of **2d** (minor product) and $[Ru(Phpy)(NCMe)_4]PF_6$, where the benzene ring has been substituted by three acetonitrile molecules [18]. In order to specifically prepare **2d**, a different strategy was chosen and a chloride abstraction from **3′** (prepared from $[Ru(\eta^6\text{-}C_6H_6)Cl_2]_2$ and 2-phenylpyridine in MeOH [40]) by silver hexafluorophosphate in acetonitrile led to pure **2d** in 70% yield. To synthesize the remaining members of the **2** series, the chloride in **3′** was easily substituted by the corresponding **a**–**c** ligands in the presence of NH_4PF_6 in MeOH and complexes **2a**–**c** were obtained in high yields (70–88%). It is worth noting that compounds **1b**, **2a** and **2c** crystallized with some amount of dichloromethane as detected by ^{1}H NMR at $\delta = 5.48$ (CD_3CN), 5.64 (acetone-d_6) and 5.44 (CD_3CN) respectively. Those chemicals shifts are in accordance with the reported values [46]. As such, the presence of dichloromethane is reflected in the obtained elemental analysis values.

3.2. X-ray diffraction studies

Single crystals suitable for X-ray diffraction were obtained for all new complexes by slow diffusion of diethylether into a dichloromethane solution. Compound **1b** crystallized with one molecule of dichloromethane. Crystallographic data, relevant bond distances and angles are summarized in Tables 1–4. The molecular structures are depicted in Figs. 2 and 3. Structure of complex **1d** has previously been reported [19], however, for the sake of comparison, crystallographic data have been included in Tables 3 and 4 All compounds adopt the expected “three-legged piano stool” structure. The distances between the nitrogen of the metalated ligand and the ruthenium center are slightly longer for the dmba derivatives than for their phpy counterparts (from 0.13 Å difference between **1a** and **2a** to 0.007 Å between **1c** and **2c**). This can be explained by the nature of the nitrogen bound to the metal, as due to the back-bonding effects, pyridines are usually more strongly bound to Ru^{II} than tertiary amines. As expected the antimony-ruthenium bonds are about 0.25 Å longer than the phosphorous-ruthenium bonds, reflecting the increase in the covalent radii from phosphorus (1.10 Å) to antimony (1.41 Å), while almost no difference is observed in the phosphorous-ruthenium bonds for complexes bearing PPh_3 or PBu_3 [45]. The average distance between the centroid of the benzene ring for all compounds is 1.72 Å, and does not vary significantly between the **1** and **2** series, albeit slightly shorter for **1d** and **2d** bearing acetonitrile ligand. These distances are consistent with those reported for similar (η^6-arene)ruthenium(II) complexes [47].

As for angles, no important difference between the two series can be noted around the ruthenium center, except for the cyclometalated nitrogen – ruthenium – E angles [E = P (**a**, **b**), Sb (**c**), N (**d**)], which are larger for dmba, from a 1.60° (**d**) difference to 10.05° (**b**). Those data probably reflect some steric repulsion between the phosphine or stibine ligands and the methyl groups of the dimethylamino substituent as the smallest difference is observed for acetonitrile and the highest for bulkier P(*n*-Bu)$_3$.

3.3. Polymerization studies

It should be noted that the complexes, particularly the cationic ones, are poorly soluble in non-polar organic solvents, and MEK was found to be the solvent of choice. The ruthenacycles are well soluble in MEK, it is non-coordinating, it allows increasing the temperature up to 80 °C and can be readily evaporated making working-up relatively straightforward. We started the investigation with polymerization of styrene, using BEB as the initiator. All complexes were evaluated in this polymerization for 6 and 24 h and the best candidates for the detailed kinetic studies were selected according to these preliminary data. The data are given in Table 5.

Table 1
Crystal structure data for complexes **1a**–**c**.

	1a	1b	1c
Empirical formula	$C_{33}H_{33}F_6NP_2Ru$	$C_{55}H_{92}Cl_2F_{12}N_2P_4Ru_2$	$C_{33}H_{33}F_6NPRuSb$
Formula weight	720.61	1406.23	811.39
Temperature (K)	298(2)	298(2)	298(2)
Wavelength (Å)	0.71073	0.71073	0.71073
Crystal system	monoclinic	triclinic	monoclinic
Space group	$P2_1/c$	*P*-1	$P2_1/c$
Unit cell dimensions (in Å and °)	$a = 11.5652(10)$	$a = 10.2217(9)$	$a = 17.650(5)$
	$b = 17.5904(14)$	$b = 12.6684(11)$	$b = 10.360(3)$
	$c = 15.4768(13)$	$c = 13.2789(12)$	$c = 18.661(5)$
	$\alpha = 90$	$\alpha = 100.2230(10$	$\alpha = 90$
	$\beta = 105.7810(10)$	$\beta = 100.5090(10)$	$\beta = 112.841(4)$
	$\gamma = 90$	$\gamma = 97.099(2)$	$\gamma = 90$
Volume (Å^3)	3029.9(4)	1642.1(3)	3144.8(15)
Z	4	1	4
Density (mg/m^3, Calcd.)	1.580	1.422	1.714
Absorption coeff. (mm^{-1})	0.685	0.708	1.450
F(000)	1464	726	1608
Crystal size (mm)	0.32 × 0.20 × 0.15	0.38 × 0.12 × 0.1	0.34 × 0.09 × 0.05
θ range for data collection (°)	1.79–25.35°	1.66 to 25.38	2.21 to 25.41
Index ranges	$-13 \le h \le 13$	$-12 \le h \le 12$	$-21 \le h \le 21$
	$-21 \le k \le 21$	$-15 \le k \le 15$	$-12 \le k \le 12$
	$-18 \le l \le 18$	$-16 \le l \le 16$	$-22 \le l \le 22$
Reflections collected	24,735	13,685	25,448
Independent reflections	5529 [R(int) = 0.0576]	6006 [R(int) = 0.0324]	5785 [R(int) = 0.0797]
Absorption correction	None	analytical	analytical
Refinement method	full-matrix least-squares on F^2	full-matrix least-squares on F^2	full-matrix least-squares on F^2
Data/Restrains/Parameters	5529/417/445	6006/530/460	5785/526/471
Goodness of fit on F^2	0.910	0.955	0.915
Final R indices [$I > 2\sigma(I)$]	$R1 = 0.0384$, $wR2 = 0.0721$	$R1 = 0.0381$, $wR2 = 0.0846$	$R1 = 0.0516$, $wR2 = 0.0991$
R indices (all data)	$R1 = 0.0574$, $wR2 = 0.0775$	$R1 = 0.0489$, $wR2 = 0.0885$	$R1 = 0.0849$, $wR2 = 0.1090$
Largest diff. peak and hole (e. Å)	0.651 and −0.372	0.491 and −0.414	3.359 and −1.054

Table 2
Crystal structure data for complexes **2a**–**d**.

	2a	2b	2c	2d
Empirical formula	$C_{35}H_{29}F_6NP_2Ru$	$C_{29}H_{41}F_6P_2Ru$	$C_{35}H_{29}F_6NPRuSb$	$C_{19}H_{17}F_6N_2PRu$
Formula weight	740.60	680.64	831.38	519.39
Temperature (K)	298(2)	298(2)	298(2)	298(2) K
Wavelength (Å)	0.71073	0.71073	0.71073	0.71073
Crystal system	monoclinic	monoclinic	monoclinic	Orthorhombic
Space group	$P2_1/c$	$P2_1/n$	$P2_1/n$	*P* b c n
Unit cell dimensions (in Å and °)	$a = 11.4000(9)$	$a = 8.7804(13)$	$a = 10.2781(12)$	$a = 15.9934(16)$
	$b = 17.2050(13)$	$b = 16.256(2)$	$b = 12.0941(14)$	$b = 16.3803(17)$
	$c = 15.9667(12)$	$c = 21.947(3)$	$c = 26.303(3)$	$c = 15.8062(16)$
	$\alpha = 90$	$\alpha = 90$	$\alpha = 90$	$\alpha = 90$
	$\beta = 97.7140(10)$	$\beta = 94.240(2)$	$\beta = 93.359(2)$	$\beta = 90$
	$\gamma = 90$	$\gamma = 90$	$\gamma = 90$	$\gamma = 90$
Volume (Å^3)	3103.3(4)	3123.9(8)	3264.0(7)	4140.9(7)
Z	4	4	4	8
Density (mg/m^3, Calcd.)	1.585	1.447	1.692	1.666
Absorption coeff. (mm^{-1})	0.671	0.659	1.399	0.894
F(000)	1496	1400	1640	2064
Crystal size (mm)	0.30 × 0.20 × 0.10	0.36 × 0.1 × 0.08	0.31 × 0.14 × 0.05	0.34 × 0.26 × 0.20
θ range for data collection (°)	1.75 to 25.35	1.86 to 25.35	1.85 to 25.35	1.78 to 25.40
Index ranges	$-13 \le h \le 13$	$-10 \le h \le 10$	$-12 \le h \le 12$	$-19 \le h \le 19$
	$-20 \le k \le 20$	$-19 \le k \le 19$	$-14 \le k \le 14$	$-19 \le k \le 19$
	$-19 \le l \le 19$	$-26 \le l \le 26$	$-31 \le l \le 31$	$-19 \le l \le 19$
Reflections collected	25,420	25,302	35,321	32,295
Independent reflections	5678 [R(int) = 0.0645]	5696 [R(int) = 0.0898]	5973 [R(int) = 0.0940]	3804 [R(int) = 0.0583]
Absorption correction	None	none	analytical	analytical
Refinement method	full-matrix least-squares on F^2	full-matrix least-squares on F^2	full-matrix least-squares on F^2	full-matrix least-squares on F^2
Data/Restrains/Parameters	5678/399/461	5696/675/474	5973/423/461	3804/1226/483
Goodness of fit on F^2	0.882	0.870	0.817	1.046
Final R indices [$I > 2\sigma(I)$]	$R1 = 0.0381$, $wR2 = 0.0673$	$R1 = 0.0483$, $wR2 = 0.0752$	$R1 = 0.0427$, $wR2 = 0.0637$	$R1 = 0.0314$, $wR2 = 0.0773$
R indices (all data)	$R1 = 0.0617$, $wR2 = 0.0730$	$R1 = 0.0958$, $wR2 = 0.0854$	$R1 = 0.0882$, $wR2 = 0.0723$	$R1 = 0.0488$, $wR2 = 0.0857$
Largest diff. peak and hole (e. Å)	0.573 and −0.330	0.662 and −0.474	0.727 and −0.371	0.231 and −0.433

Table 3
Comparison of selected bond distances [Å] between **1a**–**d** and **2a**–**d** complexes.

	1a	2a	1b	2b	1c	2c	1d [19]	2d
Ru–C_6H_6[a]	1.782	1.755	1.758	1.755	1.742	1.742	1.711	1.709
Ru–C_{met}	2.069(3)	2.058(3)	2.067(3)	2.038(5)	2.077(7)	2.063(6)	2.069(2)	2.062(3)
Ru–N_{met}	2.206(3)	2.076(3)	2.200(3)	2.074(3)	2.094(7)	2.087(5)	2.170(2)	2.081(2)
Ru–E	2.3603(9)	2.3324(9)	2.3534(9)	2.339(1)	2.5986(9)	2.5815(7)	2.058(2)	2.046(2)

E = P (**a**, **b**), Sb (**c**), N (**d**).
[a] Centroid.

Table 4
Selected angles [°] for the complexes.

	1a	2a	1b	2b	1c	2c	1d [19]	2d
N–Ru–C	78.2(1)	77.85(13)	78.30(12)	78.28(18)	78.8(3)	77.6(2)	78.10(10)	78.27(10)
N–Ru–E	95.94(7)	88.57(7)	98.85(7)	88.8(1)	91.8(3)	85.96(1)	86.65(9)	85.05(9)
C–Ru–E	85.97(8)	84.41(9)	86.35(8)	85.6(1)	82.05(17)	82.26(13)	85.98(9)	84.54(10)
C_6H_6[a]–Ru–E	126.83	132.05	123.73	130.66	126.75	131.82	126.83	129.60

E = P (**a**, **b**), Sb (**c**), N (**d**).
[a] Centroid.

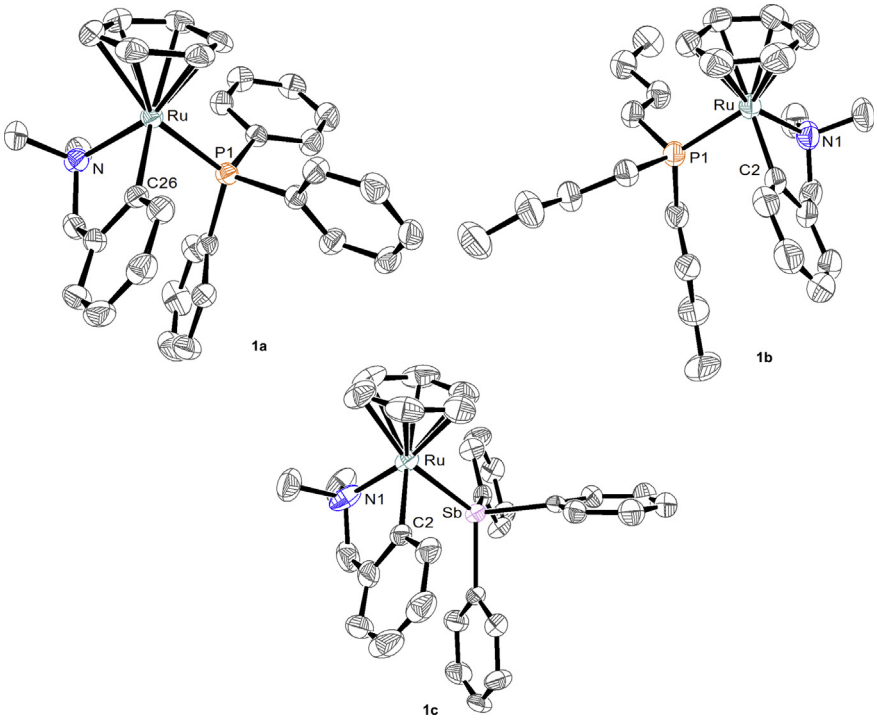

Fig. 2. ORTEP views of complexes **1a**–**c**. Thermal ellipsoids are drawn with 40% probability level. Hydrogen atoms and PF_6^- anions are omitted for clarity.

The highest conversions, above 60% in 24 h, were obtained with neutral compounds, **3′** and **3″**. The tolpy (**3″**) derivative was slightly more active but the difference in the final yields was not very significant. However, no dependence of the molecular weight on conversion was observed. Polymers of *ca*. 25,000 Da were obtained within 6 h of the reaction and this value did not change after 24 h, even if the conversion significantly increased within this period of time. Conversions reached in the polymerizations mediated by other complexes were lower, usually around 50% after 24 h with a few exceptions as described below. Thus, complexes bearing dmba (**1a**–**d**) showed quite a similar activity, resulting in around 50% polymer yields in 24 h and producing high disperse (around 2) polySt with molecular weights varying from *ca*. 15,000 to 28,000 Da. The growth of the molecular weights with conversion was observed for the polymerizations mediated by **1b** and **1d**, even if the dispersity indexes were high and the molecular weights determined by GPC were higher than the calculated values. In general, the complexes were quite active taking into account the relatively low temperature for the polymerization of St [48]. The largest difference in the catalytic performance was noted within compounds of group **2**, phpy-based ruthenacycles. The lowest polymer yields (16%) were obtained using complexes with $SbPh_3$ and relatively more labile MeCN ligands and those polymers were also characterized by the highest molecular weights (40,000 and 60,000 Da respectively). Complexes bearing phosphine ligands resulted in higher conversions after 24 h, but the polySt obtained with complex **2a** (PPh_3) displayed a very low molecular weight and high dispersity index. In fact, the most promising results were

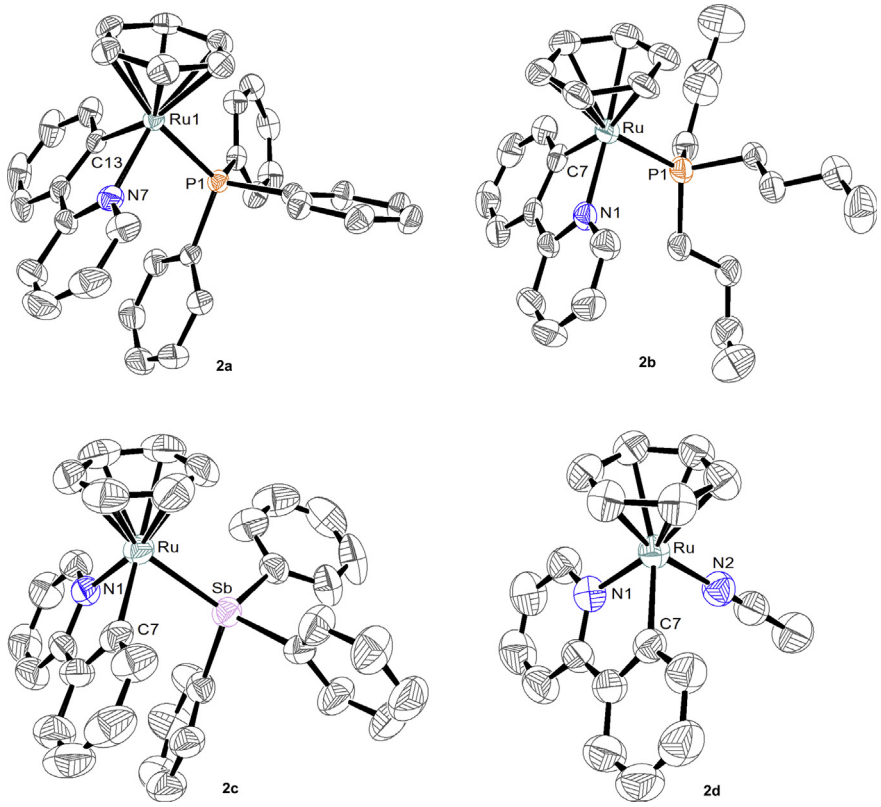

Fig. 3. ORTEP views of complexes **2a**–**d**. Thermal ellipsoids are draw with 40% probability level. Hydrogen atoms and PF_6^- anions are omitted for clarity.

Table 5
Results of the polymerization of styrene in the presence of the cyclometalated ruthenium compounds.

Complex	Time (hours)	Conversion (%)	$M_{n(GPC)}*10^{-3}$ (dalton)	$M_{n(Theo)}*10^{-3}$ (dalton)	M_w/M_n
1a	6	43.5	15.6	9.1	1.70
	24	55.0	16.6	11.5	1.97
1b	6	37.0	19.0	7.7	1.90
	24	50.0	28.3	10.4	2.36
1c	6	35.0	16.5	7.2	1.74
	24	50.5	17.4	10.5	1.90
1d	6	40.4	14.6	8.4	1.80
	24	52.5	18.4	10.9	1.72
2a	6	5.0	–	–	–
	24	20.5	2.2	4.3	2.74
2b	6	32.0	8.4	6.7	1.40
	24	46.0	10.5	9.5	1.52
2c	6	2.0	–	–	–
	24	16.4	43.5	3.3	2.38
2d	6	12.0	33.0	2.5	1.84
	24	16.5	50.6	3.4	2.47
3′	6	28.7	23.4	5.9	1.89
	24	62.9	25.9	13.2	1.99
3″	6	48.6	24.5	10.2	2.22
	24	68.2	26.1	14.2	2.31

obtained using complex with P(*n*-Bu)$_3$ ligand **2b**. The molecular weights of polySt formed in the reaction mediated by this ruthenacycle coincided well with the calculated molecular weights, and the M_w/M_n values were also the lowest in comparison with those obtained with the other complexes.

It is important to add that the radical character of the reaction was established by the stable radical (TEMPO) methodology. When 5 equivalents of TEMPO were added into the reaction mixture, no polymer was obtained after 24 h of heating. Besides, no polymerizations could be observed without the initiator, even in the presence of the ruthenacycles.

Thus taking into account these preliminary data the following complexes were selected for further investigation: cationic **1b** and **1d** from the dmba-based group as they were the only catalysts showing the growth of the molecular weights with conversion, their analogs **2b** and **2d** from phpy-based ruthenacycles, and both neutral complexes (**3′** and **3″**) as they showed the highest conversions.

The results of the kinetic measurements of polymerization with these compounds are presented in Table 6. The molecular weights

Table 6
Data on the polymerization of styrene mediated by selected complexes.

Complex	Time (hours)	Loss of initiator (%)	Conversion (%)	$M_{n(GPC)}*10^{-3}$ (dalton)	$M_{n(Theo)}*10^{-3}$ (dalton)	M_w/M_n
1	2	3	4	5	6	7
1b	1	6	–	–	–	–
	2	18	2.9	–	–	–
	3	98	24.0	15.3	5.0	1.79
	6	–	37.0	19.0	7.7	2.08
	12	–	48.8	27.0	10.2	2.09
1d	1	2	–	–	–	–
	2	16	–	–	–	–
	3	95	31.8	8.0	6.6	1.91
	6	–	40.4	14.6	8.4	1.80
	12	–	51.2	17.8	10.6	1.64
2b	1	4	–	–	–	–
	2	14	2.0	–	–	–
	3	99	18.5	5.3	3.8	2.00
	6	–	32.5	8.4	6.7	1.42
	12	–	45.0	10.5	9.4	1.39
2d	1	7	–	–	–	–
	2	19	–	–	–	–
	3	94	9.3	27.7	1.9	2.14
	6	–	12.0	33.0	2.5	2.32
	12	–	16.0	50.8	3.3	2.43
3′	1	15	4.5	–	–	–
	2	27	8.0	–	–	–
	3	50	15.2	22.8	3.2	1.96
	6	60	28.5	23.4	5.9	1.89
	12	75	46.5	23.0	9.6	1.99
3″	1	15	7.0			
	2	30	15.5			
	3	54	25.5	22.3	5.3	1.95
	6	62	46.0	24.5	9.5	2.39
	12	80	57.9	24.2	12.0	2.37

grew with conversion in the polymerizations mediated by the ionic ruthenacycles, but only in the case of **1d** and **2b** a good agreement between GPC and calculated molecular weight values was observed.

The polySt synthesized with this complex **2b** was also distinguished by narrow dispersity indexes. All these results indicate that **2b** displayed a better control of the polymerization than any other ruthenacycles involved in the study. Kinetic plot in semilogarithmic coordinates and evolution of the molecular weights with the conversion for this complex are given in Fig. 4. As one can see, the semilogarithmic plot is quite linear and the GPC curves are unimodal, relatively narrow and shifted to the higher molecular weights as the polymerization progressed. Compound **1d** also demonstrated a certain level of control in the polymerization but the difference between experimental and theoretical molecular weights was larger and the polySt was more disperse than with **2b**. Although an increase in the molecular weights of the polystyrene was observed in the process mediated by **1b**, the experimental values were about 3 times higher than the calculated ones. Conversions achieved in 12 h were similar to the conversions obtained after 24 h, meaning that the polymerizations reached a plateau in 12 h and did not progress anymore. Yields of around 50% were obtained for the polymerizations with ionic complexes, except for the process mediated by **2d**, where the conversion was very low. Polymerizations were slightly faster for the dmba based ruthenacycles than for **2b**, although the control was much better with the latter compound.

Polymerizations conducted in the presence of neutral ruthenacycles were fast but proceeded without any control, resulting in a polymer of constant molecular weight. From data depicted in Table 6, another important difference between ionic and neutral complexes could be noted. The polymerizations catalyzed by the ionic ruthenacycles clearly marked an induction period of 3 h before proceeding, meanwhile the polymerization in the presence of neutral **3′** and **3″** took place smoothly from the beginning. Interestingly, the induction time coincided very well with the consumption of the initiator in the reaction (columns 3 and 4, Table 6). During the first two hours of heating, initiator was barely consumed and the polymerizations did not occur. Abrupt disappearance of the initiator during the third hour was accompanied by initiation of the polymerization. In contrast, in polymerizations mediated by neutral group **3** compounds, the initiator was consumed gradually during the reaction time. It is logical to suppose that the cationic complexes underwent some kind of rearrangement during the induction time, converting them into active catalysts.

Loss of initiator in the polymerizations with other ionic ruthenacycles was also verified by GC. The only other complex showing a similar 3 h consumption period was **1c** with $SbPh_3$ ligand. Three other ruthenacycles behaved differently. The loss of initiator was very slow in the reaction with phpy derivatives bearing PPh_3 and $SbPh_3$ ligands, **2a** and **2c**, as practically no initiator was consumed in the first 3 h, and less than 15% after 6 h. This is in good agreement with the data on the reactions catalyzed by these complexes as no polymer was detected after 6 h. On the contrary, the initiator consumption was much faster for dmba-based ruthenacycle with PPh_3 **1a**, as almost 70% reacted during the first hour of the polymerization. However, this fast consumption was not reflected in a better controlled polymerization.

The complexes **1b** and **2b** were tested in the polymerization of VAc using the same conditions as those for styrene polymerization. In contrast to styrene, the radical derived from VAc is very active and thus forms strong bonds with the trapping end-group [49]. Despite all the progress in ATRP, no efficient catalytic system for controlled polymerization of VAc has been reported, as the vast majority of the transition metal catalysts are too “mild” to activate

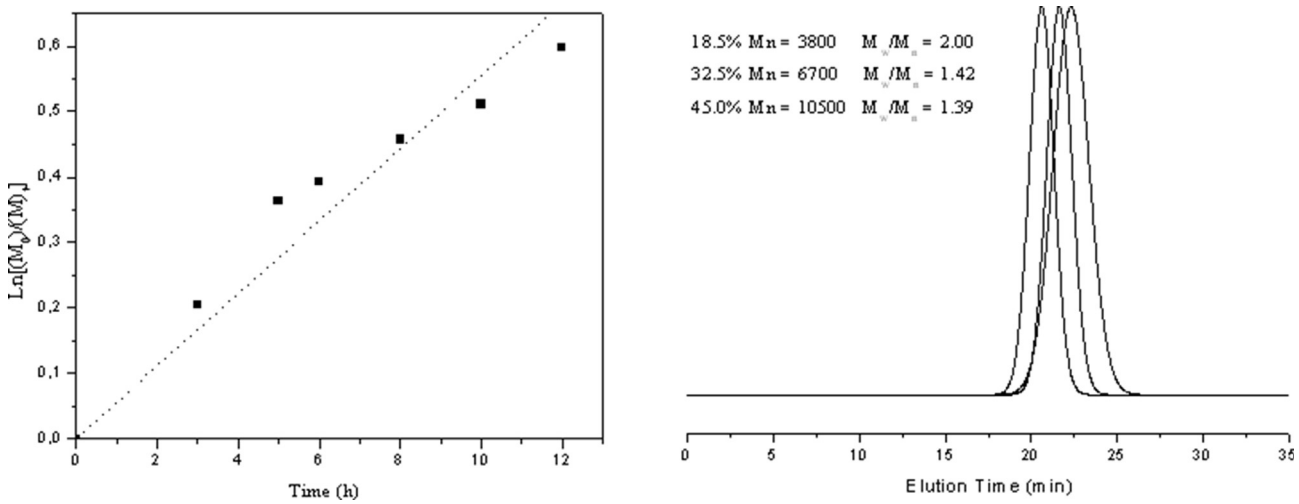

Fig. 4. (Left) Kinetic plot of polymerization of St mediated by **2b** at 80 °C in MEK (50/50 v/v) with the molar ratios of $[St]_0/[\mathbf{2b}]/[BEB]_0 = 200/1/1$; (Right) GPC traces of polySt obtained.

strongly bound C-Halogen terminals. Only a few studies on the possibility of such process have been described and one of the recent reports was based on complex **1d** which performed ATRP of VAc with moderate level of control in DMSO using CCl_4 as initiator [37,50]. Although the polymerization did not proceed to high conversions and the M_w/M_n values were not low enough, the participation of the ATRP mechanism in the process could be demonstrated. In the present study, an attempt has been made to expand the number of potential candidates for such important catalytic process. Nevertheless, none of complexes **1b** and **2b** were active in BEB initiated polymerization of VAc in MEK at 80 °C, *i.e.* under the conditions used for styrene. However, when CCl_4 was utilized instead of BEB, polymerization of VAc was observed with complex **1b**. The reaction resulted in a maximum of *ca.* 30% conversion in 12 h and polyVAc of monomodal weight distribution with $M_{n,GPC} = 8500$ Da and $M_w/M_n = 1.45$. Interestingly, the constant growth of the molecular weights was observed, as well as the decrease of M_w/M_n values with the conversion. Since CCl_4 was also consumed slowly (50% in 3 h and 80% in 6 h), the reaction most probably proceeded via a red-ox initiation catalyzed by **1d**, with CCl_4 acting as initiator and chain transfer agent [37]. However, participation of the ATRP mechanism could not be completely excluded in this case. For comparison, complex **1d** under these conditions resulted in a maximum of 15% conversion, producing low molecular weight (5000 Da) polyVAc. Thus, complex **1b** may be more promising for the living/controlled polymerization of VAc than **1d**, but thorough investigation of the mechanism and search for optimal conditions are required.

3.4. Mechanistic studies

As no clear conclusion could be drawn from the results described above and in order to understand what kind of reaction may occur during the initial period of the polymerization of styrene, the stoichiometric reaction between BEB (initiator) and all the ionic ruthenium complexes was investigated at 80 °C by ^{1}H NMR spectroscopy and practically no changes were noted after 3 h, except for complex **1a**. Therefore, the reaction of **1a** with BEB was studied in more details and its behavior was compared with that of **2a**.

An interesting reaction took place when complex **1a** was heated to 80 °C in MEK for 3 h. A red precipitate was observed, which was filtered off (45% yield) and analyzed by ^{1}H and ^{31}P NMR. Spectra showed that the signals corresponding to the dmba moiety had disappeared and a new signal appeared in ^{31}P NMR at 23.6 ppm. Comparison with the data obtained from a pure sample prepared accordingly to the literature [41,42] showed that the coordination of two bromides from the initiator took place, leading to the formation of neutral $[Ru(\eta^6\text{-}C_6H_6)Br_2(PPh_3)]$ complex **4** (Fig. 5). Analysis by GC/MS of the remaining solution after filtration of **4** only showed the presence of *N*,*N*-dimethylbenzylamine, residual BEB and 1-phenylethanol, probably arising from the hydrolysis of BEB. No coupling products from BEB and dmba could be detected. Under the same condition, complex **2a** did not react with BEB. We previously reported the relative fragility of dmba complexes *versus* their phpy analogs and the cleavage of the Ru–C σ bond of **1d** by MeOH with the concomitant arene substitution by 2,2′-bipyridine

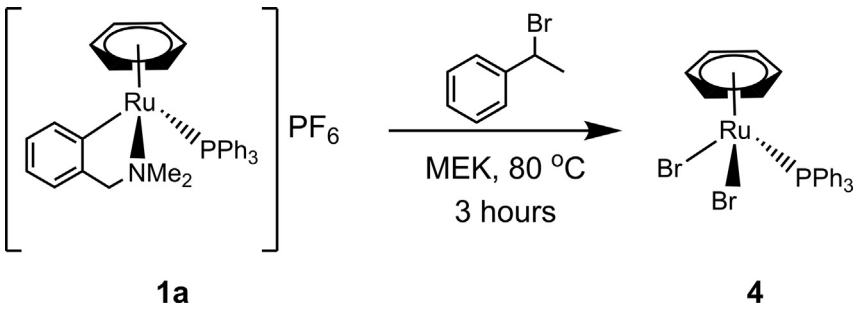

Fig. 5. Reaction between complex **1a** and the BEB initiator.

[8]. When compound **4** was used in the polymerization of styrene under the same conditions as described above, no polymer could be detected after 24 h, allowing to discard the hypothesis that **4** is the active catalyst formed during the induction period.

In another series of reactions, complex **2a** was reacted with five equivalents of styrene in $(CD_3)_2CO$ at 80 °C in a sealed tube, and the reaction was monitored by ^1H and ^{31}P NMR. After 24 h, most of the complex remained intact (approx. 80%), but some new peaks arose. Significantly, in ^{31}P NMR a new signal appeared at 22.65 ppm and in ^1H NMR a signal at 7.34 ppm could be attributed to free benzene, and new features were detected at 6.48 (dd), 6.42 (dd) and 5.23 (d) ppm. Other new peaks are masked by those of **2a** and styrene. This observation suggests that styrene could be coordinated to the ruthenium center, as the observed chemical shifts are in accordance with the data reported for (η^6-styrene)ruthenium complexes [51,52]. The low yield after 24 h can be explained by the 1:5 (Ru:St) stoichiometry of the reaction. Under the polymerization conditions the Ru:St relation is 1:200, which could lead to a faster and more quantitative reaction, as arene exchange on ruthenium(II) complexes usually takes place with a large excess of the incoming ligand at high temperatures [53]. Thus, an arene exchange reaction could explain the low catalytic activity displayed by the complexes. However, those are preliminary results and more work is needed in order to isolate the new complex and confirm the coordination of styrene.

4. Conclusions

A series of [Ru(η^6-C_6H_6)(N∩C)L]PF_6 isomorphous half-sandwich complexes, bearing cyclometalated dmba (**1a**–**d**) and phpy (**2a**–**d**) moieties, has readily been prepared by ligand substitution in high yields. The comparative catalytic activity of the complexes in the radical polymerization of styrene and vinyl acetate has been studied. However, no direct correlation between the catalyst structure and its catalytic activity could be drawn. The complexes of the dmba group showed good activity in the polymerization of styrene but only with two of them, **1b** (P(*n*-Bu)$_3$) and **1d** (MeCN), a growth of the molecular weight with conversion was observed. Complexes of the phpy group were much less active, except for **2b**. Although the polymerization of styrene with this complex was somewhat slower, a good coincidence between the experimental and calculated molecular weights was found, meaning a better controlled process. Kinetic studies revealed an induction period in the polymerization of styrene mediated by ionic complexes. The induction period coincides with the complete consumption of the initiator, suggesting some rearrangement in the coordination sphere of the complexes converting them into active catalysts. Such gradual rearrangement may be responsible for the high dispersity indexes of the obtained polySt. As for the polymerization of vinyl acetate, only complex **1b** with P(*n*-Bu)$_3$, was active, providing CCl_4 is used as initiator. Interestingly, the complexes exhibiting the best control/activity behavior, **2b** in the polymerization of St and **1b** in the polymerization of VAc, contain the P(*n*-Bu)$_3$ ligand. According to Tolman [54], P(*n*-Bu)$_3$ is more electron donating and less bulky than the much more commonly used PPh_3, making worth investigating the contribution of such parameters in the mechanism of ATRP and related reactions catalyzed by ruthenium(II) species. On the other hand, displacement of the metalated dmba fragment by bromides from the initiator was observed, but the resulting neutral species did not catalyze the polymerization, suggesting that more robust phpy ligand may be preferable.

Acknowledgments

Financial support from CONACyT (Projects 153151 and 129801, and scholarship 6758 to V. Martinez Cornejo) is gratefully acknowledged. The authors thank Gerardo Cedillo Valverde (Instituto de Investigaciones en Materiales) and María de la Paz Orta Pérez (Instituto de Química) for the support in NMR and elemental analysis measurements. We wish to dedicate this contribution to the memory of Professor Armando Cabrera Ortiz (1944–2014).

Appendix A. Supplementary material

CCDC 1420624 (**1a**), 1420625 (**1b**), 1420626 (**1c**), 1420627 (**2a**), 1420628 (**2b**), 1420629 (**2c**) and 1420630 (**2d**) contain the supplementary crystallographic data for the new compounds. These data can be obtained free of charge from the Cambridge Crystallographic data Center via www.ccdc.cam.ac.uk/data_request/cif.

References

[1] J.-P. Djukic, J.-B. Sortais, L. Barloy, M. Pfeffer, Eur. J. Inorg. Chem. (2009) 817–853.
[2] M. Albrecht, Chem. Rev. 110 (2010) 576–623.
[3] A.D. Ryabov, Chem. Rev. 90 (1990) 403–424.
[4] Palladacycles: Synthesis, Characterization and Applications, John Wiley & Sons, 2008.
[5] S.H. Wadman, J.M. Kroon, K. Bakker, M. Lutz, A.L. Spek, G.P.M. van Klink, G. van Koten, Chem. Commun. 4 (2007) 1907.
[6] T. Bessho, E. Yoneda, J.-H. Yum, M. Guglielmi, I. Tavernelli, H. Imai, U. Rothlisberger, M.K. Nazeeruddin, M. Grätzel, J. Am. Chem. Soc. 131 (2009) 5930–5934.
[7] J.-P. Launay, Chem. Soc. Rev. 30 (2001) 386–397.
[8] A.D. Ryabov, V.S. Sukharev, L. Alexandrova, R. Le Lagadec, M. Pfeffer, Inorg. Chem. 40 (2001) 6529–6532.
[9] A.D. Ryabov, V.S. Kurova, E.V. Ivanova, R. Le Lagadec, L. Alexandrova, Anal. Chem. 77 (2005) 1132–1139.
[10] E.V. Ivanova, I.V. Kurnikov, A. Fischer, L. Alexandrova, A.D. Ryabov, J. Mol. Catal. B Enzym 41 (2006) 110–116.
[11] A.D. Ryabov, Adv. Inorg. Chem. 55 (2004) 201–269.
[12] H. Huang, P. Zhang, H. Chen, L. Ji, H. Chao, Chem. – A Eur. J. 21 (2015) 715–725.
[13] B. Peña, A. David, C. Pavani, M.S. Baptista, J.P. Pellois, C. Turro, K.R. Dunbar, Organometallics 33 (2014) 1100–1103.
[14] L. Leyva, C. Sirlin, L. Rubio, C. Franco, R. Le Lagadec, J. Spencer, P. Bischoff, C. Gaiddon, J.P. Loeffler, M. Pfeffer, Eur. J. Inorg. Chem. (2007) 3055–3066.
[15] L.N. Lewis, J.F. Smith, J. Am. Chem. Soc. 108 (1986) 2728–2735.
[16] P. Dani, T. Karlen, R.A. Gossage, S. Gladiali, G. Van Koten, Angew. Chem. Int. Ed. Engl. 39 (2000) 743–745.
[17] W. Baratta, P. Da Ros, A. Del Zotto, A. Sechi, E. Zangrando, P. Rigo, Angew. Chem. Int. Ed. Engl. 43 (2004) 3584–3588.
[18] S. Fernandez, M. Pfeffer, V. Ritleng, C. Sirlin, Organometallics 18 (1999) 2390–2394.
[19] R. Le Lagadec, L. Rubio, L. Alexandrova, R.A. Toscano, E.V. Ivanova, R. Meškys, V. Laurinavičius, M. Pfeffer, A.D. Ryabov, J. Organomet. Chem. 689 (2004) 4820–4832.
[20] B. Boff, M. Ali, L. Alexandrova, N.A. Espinosa-Jalapa, R.O. Saavedra-Díaz, R. Le Lagadec, M. Pfeffer, Organometallics 32 (2013) 5092–5097.
[21] A.S. Lima-Barbosa, C. Werlé, C.O. Colunga-Oliva, C. Franco-Rodríguez, R.A. Toscano, R. Le Lagadec, M. Pfeffer, Inorg. Chem. 54 (2015) 7617–7626.
[22] M. Kato, M. Kamigaito, M. Sawamoto, T. Higashimuras, Macromolecules 28 (1995) 1721–1723.
[23] M. Ouchi, T. Terashima, M. Sawamoto, Chem. Rev. 109 (2009) 4963–5050.
[24] Y. Borguet, A. Richel, S. Delfosse, A. Leclerc, L. Delaude, A. Demonceau, Tetrahedron Lett. 48 (2007) 6334–6338.
[25] K. Severin, Chimia 66 (2012) 386–388.
[26] K. Parkhomenko, L. Barloy, J.B. Sortais, J.P. Djukic, M. Pfeffer, Tetrahedron Lett. 51 (2010) 822–825.
[27] W.A. Braunecker, N.V. Tsarevsky, A. Gennaro, K. Matyjaszewski, Macromolecules 42 (2009) 6348–6360.
[28] T. Ando, M. Kamigaito, M. Sawamoto, Macromolecules 33 (2000) 5825–5829.
[29] A. Richel, A. Demonceau, A.F. Noels, Tetrahedron Lett. 47 (2006) 2077–2081.
[30] C. Aguilar-Lugo, R. Le Lagadec, A.D. Ryabov, G.C. Valverde, S. Lopez-Morales, L. Alexandrova, J. Polym. Sci. Part A Polym. Chem. 47 (2009) 3814–3828.
[31] M. Beley, S. Chodorowski-Kimmes, J.-P. Collin, P. Lainé, J.-P. Launay, J.-P. Sauvage, Angew. Chem. Int. Ed. Engl. 33 (1994) 1775–1778.
[32] T. Koizumi, T. Tomon, K. Tanaka, Organometallics (2003) 970–975.
[33] C. Moorlag, M.O. Wolf, C. Bohne, B.O. Patrick, J. Am. Chem. Soc. 127 (2005) 6382–6393.
[34] N. Vargas-Alfredo, N. Espinosa-Jalapa, S. Lopez-Morales, A.D. Ryabov, R. Le Lagadec, L. Alexandrova, Macromolecules 45 (2012) 8135–8146.
[35] N. Vargas-Alfredo, C. Aguilar-Lugo, O. Gonzalez-Diaz, R. Le Lagadec, L. Alexandrova, Macromol. Symp. 325–326 (2013) 10–20.
[36] M.O. Gonzalez-Diaz, S. Lopez-Morales, R. Le Lagadec, L. Alexandrova, J. Polym.

Sci. Part A Polym. Chem. 49 (2011) 4562–4577.
[37] J. Olvera-Mancilla, S. López-Morales, J. Palacios-Alquisira, D. Morales-Morales, R. Le Lagadec, L. Alexandrova, Polymer 55 (2014) 1656–1665.
[38] L. Quebatte, R. Scopelliti, K. Severin, Eur. J. Inorg. Chem. 2 (2005) 3353–3358.
[39] B. De Clercq, F. Verpoort, Polym. Bull. 50 (2003) 153–160.
[40] O. Saavedra-Díaz, R. Cerón-Camacho, S. Hernández, A.D. Ryabov, R. Le Lagadec, Eur. J. Inorg. Chem. (2008) 4866–4869.
[41] R.A. Zelonka, M.C. Baird, Can. J. Chem. 50 (1972) 3063–3072.
[42] R.A. Zelonka, M.C. Baird, J. Organomet. Chem. 44 (1972) 383–389.
[43] AXS, SAINT, Software Reference Manual, Bruker, Madison, WI, 1998.
[44] G.M. Sheldrick, SHELXS-2012 and SHELXL-2014/7, University of Gottingen, Germany.
[45] W. Levason, G. Reid, Coord. Chem. Rev. 250 (2006) 2565–2594.
[46] G.R. Fulmer, A.J.M. Miller, N.H. Sherden, H.E. Gottlieb, A. Nudelman, B.M. Stoltz, J.E. Bercaw, K.I. Goldberg, Organometallics 29 (2010) 2176–2179.
[47] J.G. Małecki, M. Jaworska, R. Kruszynski, J. Kłak, Polyhedron 24 (2005) 3012–3021.
[48] M. Kamigaito, T. Ando, M. Sawamoto, Chem. Rev. 101 (2001) 3689–3745.
[49] G. Moad, D.H. Solomon, The Chemistry of Radical Polymerization, Elsevier, 2005.
[50] M. Wakioka, K.-Y. Baek, T. Ando, M. Kamigaito, M. Sawamoto, Macromolecules 35 (2002) 330–333.
[51] M.A. Bennett, H. Neumann, M. Thomas, X. Wang, Organometallics 10 (1991) 3237–3245.
[52] D.W. Lee, C.S. Yi, Organometallics 29 (2010) 3413–3417.
[53] M.A. Bennett, T.-N. Huang, T.W. Matheson, A.K. Smith, Inorg. Synth. 21 (1982) 74.
[54] C.A. Tolman, Chem. Rev. 77 (1977) 313–348.